



MG53 Does Not Manifest the Development of Diabetes in *db/db* Mice

Qiang Wang,¹ Zehua Bian,¹ Qiwei Jiang,¹ Xiaoliang Wang,¹ Xinyu Zhou,¹ Ki Ho Park,¹ Willa Hsueh,² Bryan A. Whitson,¹ Erin Haggard,¹ Haichang Li,¹ Ken Chen,^{3,4} Chuanxi Cai,¹ Tao Tan,^{1,5} Hua Zhu,¹ and Jianjie Ma¹

Diabetes 2020;69:1052–1064 | <https://doi.org/10.2337/db19-0807>

MG53 is a member of the TRIM protein family that is predominantly expressed in striated muscles and participates in cell membrane repair. Controversy exists regarding MG53's role in insulin signaling and manifestation of diabetes. We generated *db/db* mice with either whole-body ablation or sustained elevation of MG53 in the bloodstream in order to evaluate the physiological function of MG53 in diabetes. To quantify the amount of MG53 protein in circulation, we developed a monoclonal antibody against MG53 with high specificity. Western blot using this antibody revealed lower or no change of serum MG53 levels in *db/db* mice or patients with diabetes compared with control subjects. Neither whole-body ablation of MG53 nor sustained elevation of MG53 in circulation altered insulin signaling and glucose handling in *db/db* mice. Instead, mice with ablation of MG53 were more susceptible to streptozotocin-induced dysfunctional handling of glucose compared with the wild-type littermates. Alkaline-induced corneal injury demonstrated delayed healing in *db/db* mice, which was restored by topical administration of recombinant human (rh)MG53. Daily intravenous administration of rhMG53 in rats at concentrations up to 10 mg/kg did not produce adverse effects on glucose handling. These findings challenge the hypothetical function of MG53 as a causative factor for the development of diabetes. Our data suggest that rhMG53 is a potentially safe and effective biologic to treat diabetic oculopathy in rodents.

Diabetes is a leading economic and social burden worldwide. It has been estimated that 422 million adults are living with diabetes, with direct annual costs of more than \$827 billion (1–3). As a result of hyperglycemia, hyperlipidemia, and impaired regenerative capacity in patients with diabetes, a wide range of complications have been commonly found, including heart attacks, strokes, defects in wound healing, and vision loss (4). Thus, identifying key molecules for improving regenerative capacity is critical for developing effective treatments for these diabetes-induced complications.

We previously identified a protein, mitsugumin 53 (MG53), as a main component for plasma membrane repair machinery (5). An extensive series of subsequent studies established that recombinant human (rh)MG53 protein can be used to treat injuries to multiple organs, including skeletal muscle, heart, lung, kidney, brain, cornea, and skin (6–13). Many of these organs are also impacted by long-standing diabetes, suggesting that MG53 may be an ideal therapeutic agent for treating multiorgan damage in diabetes. However, one group's recent publications suggest that overexpression of MG53 is a causative factor for diabetes by promoting insulin receptor substrate-1 (IRS-1) degradation (14), inducing lipid toxicity (15), and blocking insulin binding to its receptor (16).

In this study, we tested the hypothesis that MG53 has the potential to treat diabetes-related tissue injuries without impacting insulin action or glucose handling. One

¹Department of Surgery, The Ohio State University Wexner Medical Center, Columbus, OH

²Diabetes and Metabolism Research Center, Department of Internal Medicine, The Ohio State University Wexner Medical Center, Columbus, OH

³Department of Cardiology, The General Hospital of Western Theater Command, Chengdu, Sichuan, China

⁴Department of Cardiology, Daping Hospital, The Third Military Medical University, Chongqing, China

⁵TRIM-edicine, Inc., Columbus, OH

Corresponding authors: Jianjie Ma, jianjie.ma@osumc.edu, Hua Zhu, hua.zhu@osumc.edu, and Tao Tan, ttan@trim-edicine.com

Received 14 August 2019 and accepted 25 February 2020

This article contains Supplementary Data online at <https://diabetes.diabetesjournals.org/lookup/suppl/doi:10.2337/db19-0807/-/DC1>.

Q.W., Z.B., and Q.J. contributed equally to this work.

© 2020 by the American Diabetes Association. Readers may use this article as long as the work is properly cited, the use is educational and not for profit, and the work is not altered. More information is available at <https://www.diabetesjournals.org/content/license>.

challenge with the study of MG53 is the development and validation of antibody that can be used to quantify the protein level of MG53 in tissue and serum. Here, we developed a highly sensitive and specific monoclonal MG53 antibody and found that MG53 expression in skeletal muscle of diabetic animals and healthy controls is similar, which is consistent with findings from multiple research groups (17–23). However, we found that circulating MG53 is significantly reduced in blood samples from diabetic mice compared with those from wild-type (WT) littermates, which is in contrast to the recent study by Wu et al. (16), who reported elevated MG53 in blood samples derived from the *db/db* mice. To determine the role of MG53 in diabetes, we generated *db/db* mice with either whole-body ablation or sustained elevation of MG53 in the bloodstream. We found no evidence of altered glucose handling and insulin signaling in these mice models. Instead, we found that streptozotocin (STZ) treatment of the *mg53*^{-/-} mice caused abnormal glucose handling indicative of MG53's protective role in β -cell function. We also used rhMG53 to treat alkaline-induced corneal wounds and found that topical application of rhMG53 significantly improved corneal wound healing defects in diabetic mice. Thus, MG53 is a potential therapeutic agent to treat diabetes-related tissue injuries because it does not impact insulin action or glucose disposal.

RESEARCH DESIGN AND METHODS

Experimental Animals

MG53 knockout mice (*mg53*^{-/-}), originally created in the Sv129/C57BL/6 mixed genetic background (5), were backcrossed with the Sv129 or C57BL/6 mice for more than eight generations to create two additional mouse strains with knockout of MG53, e.g., Sv129-*mg53*^{-/-} and C57BL/6-*mg53*^{-/-}. *db/db-mg53*^{-/-} mice were generated by crossing *mg53*^{-/-} with *db/db*^{+/-} mice. *mg53*^{-/-} mice and *db/db*^{+/-} mice were bred to generate F1 founder mice with genotype of *db/db*^{+/-}-*mg53*^{+/-}. Then, the F1 founder mice were bred to generate *mg53*^{+/+}/*db/db*^{+/+} (WT), *mg53*^{-/-}/*db/db*^{+/+} (*mg53*^{-/-}), and *mg53*^{+/+}/*db/db*^{-/-} (*db/db*) littermates for experimentation. The pups were genotyped using our established methods for *mg53*^{-/-} (5) and *db/db* (24). *db/db*-tPA-MG53 mice were generated by crossing the tPA-MG53 mice (12) with *db/db*^{+/-} mice. To minimize potential variations associated with the different genetic backgrounds, we conducted all experiments (growth rate, glucose tolerance test [GTT], and insulin tolerance test [ITT] tests) using the littermate mice. Mice were fed with standard chow diet from Envigo (Teklad irradiated LM-485 mouse/rat diet, cat. no. 7912-102819M).

Development of a Rabbit Monoclonal MG53 Antibody

The rabbit monoclonal anti-MG53 antibody, mAb-MG53, was generated through custom order by Epitomics. Briefly, rabbits were immunized by rhMG53. Through fusion

of the spleen cells derived from the immunized rabbits and rabbit plasmacytomas, a pool of hybridoma clones was generated. We screened several stable hybridoma clones that secreted anti-MG53 antibodies. The clone used in the current study, mAb-MG53, has the highest sensitivity and has been validated in our previous publications (8,9,13,25).

Immunoblotting

Muscle lysates were separated by 10% SDS-PAGE and transferred onto polyvinylidene fluoride membranes (Millipore). The blots were washed with Tris-buffered saline Tween-20 (TBST), blocked with 5% milk in TBST for 1 h, and incubated with custom-made mAb-MG53 or commercial Abcam anti-MG53 antibody (cat. no. 83302). Different amounts of rhMG53 were loaded as positive controls. Immunoblots were visualized with an ECL Plus kit (Pierce).

Serum MG53 Quantification

For Western blot (WB), different amounts of rhMG53 (0.2, 0.1, and 0.05 ng) mixed with 1 μ L serum from *mg53*^{-/-} mice were loaded onto the 8.7% SDS-PAGE gel and served as a reference standard. Serum samples from WT mouse were loaded with volumes of 1 μ L or 2 μ L and probed with mAb-MG53 or Abcam anti-MG53 antibody. The density of the WB was plotted against the rhMG53 standard concentrations, and regression analysis was used to calculate the concentration of MG53 in serum derived from the WT and *db/db* serum.

Immunofluorescent Staining

Tissue samples were fixed in 4% paraformaldehyde overnight at 4°C. After fixation, samples were washed three times for 5 min with 70% ethanol. Washed samples were processed and embedded in paraffin. Immunofluorescent staining of CD31 was performed using flat mount corneas following a previously published study (13,26). Paraffin section (4 μ m thick) were cut as slides for immunofluorescent staining, which was performed as follows: slides were deparaffinized and rehydrated by incubating successively in xylene; 100%, 95%, 75%, and 50% ethanol; and PBS. Antigen retrieval was achieved by heating in the pressure cooker with Tris-EDTA buffer for 13 min. Primary antibodies were applied and incubated at 4°C overnight. DAPI was used to stain the nucleus of the tissue. All images were captured by a Zeiss LSM 780 confocal microscope and analyzed by ImageJ.

Soleus Muscle Insulin Stimulation

Soleus muscles derived from WT and *db/db* mice were challenged with insulin (10 units/L, in Krebs solution) following the published protocol (16). The incubation solution was collected at 0, 15, 30, 60, and 120 min after insulin treatment. Then the solution samples were concentrated by Amicon Centrifugal Filter Units and subjected to WB analysis for MG53.

Animal Care and In Vivo Corneal Wound Healing Models

A 2-mm filter paper disc soaked in 1 N NaOH was applied to the axial cornea to induce injury. Fourteen days post-alkaline injury, the mice were sacrificed and eyes underwent analyses. In order to obtain details regarding the injury response in WT and *db/db* corneas, globes were fixed either for horizontal sectioning or for flat mount staining. Analysis of all tissues was performed by an individual masked to the genotype. For rhMG53 treatment of corneal wounds, wounded corneas received topical sterile saline with 0 or 100 ng/mL rhMG53 for 30 μ L/eye daily for a total of 14 days. Size and depth of the corneal wound were verified daily using fluorescein. At 14 days following treatment, animals were euthanized and globes were enucleated. In all subsequent histologic analyses, the individual was masked to the treatment.

STZ Induced Acute Diabetes in Mice

WT and *mg53*^{-/-} littermate mice (male, 5 months old) were administered five doses of STZ by intraperitoneal (i.p.) injection to induce acute type 1 diabetes, according to the protocol of Nicholas et al. (27). STZ was prepared freshly each day (dissolved in 50 mmol/L citrate buffer, pH 4.5) and administered to mice for five consecutive days (40 mg/kg body wt per dose). One and two weeks following the last injection, the mice were fasted for 6 h and fasting blood glucose levels were measured.

GTT

Following fasting (15-h deprivation of diet: 6:00 P.M. to 9:00 A.M.), mice were injected with a bolus of glucose (1 g/kg i.p., 10% D-glucose, freshly prepared in sterile 0.9% NaCl solution). Blood glucose from mouse tail vein was assessed at 15, 30, 45, 90, and 120 min after glucose administration.

Insulin Tolerance Test

Mice were singly housed and fasted for 6 h prior to test. Following fasting, mice were injected with a bolus of insulin (0.75 units/kg i.p.) (insulin was freshly prepared in sterile 0.9% NaCl solution; Sigma-Aldrich). Blood glucose was assessed at 10, 25, 45, 90, and 120 min after insulin administration.

Repeat Dose Toxicity Study of rhMG53 in Sprague-Dawley Rats

Male and female Sprague-Dawley rats (three per sex) were given an intravenous bolus injection via tail vein over \sim 1 min every 2 days for a 14-day period (seven total dose administrations) of rhMG53 at 1, 10, and 40 mg/kg. A control group, three per sex, was given vehicle (Sterile Water for Injection, USP) at an equivalent volume by the same administration regimen. Animals were sacrificed on day 14. These studies were conducted by a contract research organization (SRI Bioscience, Menlo Park, CA) in accordance to U.S. Food and Drug Administration guidance.

Human Serum Sample Collection

Peripheral venous blood samples were collected between 6:00 and 7:00 A.M. after overnight fasting and kept at room temperature for clotting and centrifuged at 3,000g for 15 min to obtain serum. Serum fasting blood glucose was measured by an automatic chemistry analyzer (Beckman Coulter, Inc., Brea, CA). Vital data for the individual patients are listed in Table 1.

Statistical Analysis

The data are represented as means \pm SD. Comparisons were made by Student *t* test for comparison of two experimental groups and by ANOVA for repeated measures. The SD of the mean is indicated by error bars for each group of data. Area under curve (AUC) for the GTT tests was calculated by Prism 7 software. A value of *P* < 0.05 was considered significant. All of these data were analyzed using Prism 7 software.

Data and Resource Availability

All data generated or analyzed during this study are included here in the published article. The animal models and antibody generated in this study will be made available to the research community upon request.

RESULTS

High-Sensitivity MG53 Antibody Detects Lower Level of MG53 in Sera Derived from *db/db* Mice

Identification and quantification of MG53 protein in serum and tissue samples require the development of a sensitive antibody with high specificity. We previously obtained rhMG53 protein with >98% purity from *Escherichia coli* fermentation. Immunization of rabbit with rhMG53 produced a pool of monoclonal antibodies (mAbs) that recognized MG53 in broader animal species including mice and humans. Out of the mAb pool, we identified one clone with high specificity and high sensitivity, mAb-MG53, to detect MG53 in both WB and immunohistochemical (IHC) staining. As shown in Fig. 1A, IHC staining of skeletal muscle and cardiac muscle derived from mice showed a clear subcellular distribution pattern of MG53 in the cytosol and on the plasma membrane. In particular, MG53 protein was found to concentrate in the

Table 1—Baseline characteristics of the participants in control and diabetes groups

Parameters	Control (n = 10)	Diabetes (n = 10)	<i>P</i>
Sex (male:female)	10:0	6:4*	0.043
Age (years)	72 (61–74)	66 (60–68)	0.378
FBG (mmol/L)	4.72 (4.02–5.01)	6.81 (5.20–12.98)*	0.007
HbA _{1c} (%)	N/A	7.11 \pm 1.05	N/A

Age and fasting blood glucose (FBG) are presented as median and quartiles. HbA_{1c} is mean \pm SD. **P* < 0.05 vs. control. *P* values are from two-tailed tests.

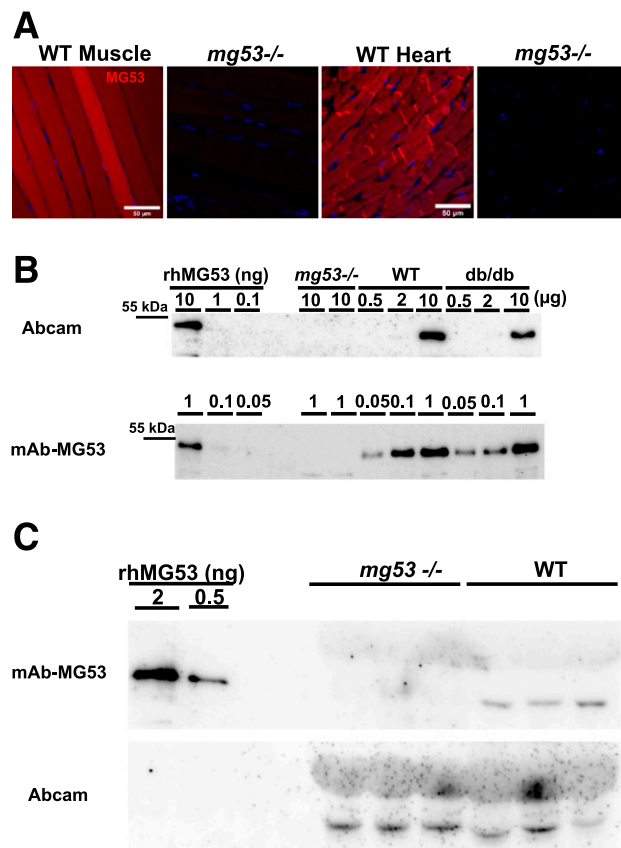


Figure 1—Commercially available antibody against MG53 detects nonspecific band in serum derived from *mg53*^{-/-} mice. **A:** IHC of MG53 with mAb-MG53 in muscle and heart derived from WT and *mg53*^{-/-} mice. **B:** WB of muscle samples derived from *mg53*^{-/-}, WT, and *db/db* mice. Smaller amounts of muscle sample (0.05–1.00 μg [bottom]) were used to show high sensitivity of mAb-MG53 compared with greater amounts of muscle samples (0.5–10.0 μg) used for WB with Abcam antibody (cat. no. 83302). Various amounts of rhMG53 protein dissolved in the running buffer were used as reference standards. **C:** Sera derived from *mg53*^{-/-} and WT littermates (1 μL per lane; each lane represents a different mouse) were first probed with mAb-MG53 (top). The membrane was stripped and then probed with the Abcam antibody (bottom).

gap junction of mouse cardiomyocytes. This antibody can detect low levels of MG53 protein in human heart (28). Specificity of mAb-MG53 is shown in the negative staining of muscle and heart samples derived from the *mg53*^{-/-} mice.

Compared with the commercially available antibodies, our mAb-MG53 has >20-fold increased sensitivity. Specifically, the Abcam antibody (cat. no. 83302) that was used by Wu et al. (16) required 10-fold higher loading of muscle samples for detection of MG53 protein in WT and *db/db* mice (Fig. 1B). To compare the differential sensitivity of our mAb-MG53 and the commercial Abcam antibody, we performed WB using the same membrane loaded with varying amounts of the skeletal muscle samples derived from the WT mice. The result, presented in Supplementary Fig. 1, demonstrated that under identical imaging conditions, detection of the MG53 signal with the Abcam antibody required loading of 10 μg muscle sample,

whereas only 0.2 μg muscle sample loading was required for detection of the MG53 signal using our mAb-MG53 antibody.

In addition, we used this mAb-MG53 to detect and quantify MG53 protein levels in sera derived from mice from three different genetic backgrounds: brown, Sv129/C57BL/6; white, Sv129; and black, C57BL/6. As shown in Supplementary Fig. 2, serum samples derived from the *mg53*^{-/-} mice were negative for mAb-MG53. Surprisingly, the Abcam antibody that was used by Wu et al. (16) could detect a band at ~48–53 kDa, but such band is also present in all three strains of mice with knockout of MG53. The nonspecific band recognized by the Abcam antibody could not be detected by our mAb-MG53 antibody. This mAb-MG53 antibody has been used previously, both for WB and immunohistochemistry staining (28). Cross-reactivity of the Abcam antibody was clearly seen in Fig. 1C, using the same membrane first probed with mAb-MG53 and then stripped and reprobed with the Abcam antibody. The sera derived from the *mg53*^{-/-} mice were negative for mAb-MG53 (Fig. 1C, top). Unexpectedly, a band of ~48 kDa was visible in the *mg53*^{-/-} sera when reprobed with the Abcam antibody (Fig. 1C, bottom).

We explored the linearity range of the mAb-MG53 by loading varying concentrations of rhMG53 in WB, which allowed us to quantify the basal level of MG53 in mouse serum to be in the range of 30–50 ng/mL (Fig. 2A). This may be an underestimate of the level of MG53 in mouse serum considering the antibody was generated using human MG53 protein as an antigen. However, it was still ~100-fold higher than the level reported by Wu et al. (16) (see Fig. 3C in the article by Wu et al.). We obtained littermates of WT and *db/db* mice from The Jackson Laboratory and assessed the serum level of MG53 using WB (Fig. 2B). Data from multiple animals are summarized in Fig. 2C and which showed significantly lower levels of MG53 in the *db/db* serum compared with the WT littermates. This finding is in sharp contrast to the report by Wu et al. (16), which showed approximately onefold higher levels of MG53 protein in the *db/db* serum with use of the Abcam antibody and their custom-made antibody.

We obtained a limited number of human serum samples derived from volunteers without diabetes and patients with diabetes. As shown in Fig. 2D, large variations in MG53 protein levels were detected in both samples of those without diabetes and samples of those with diabetes, likely reflecting the varying degrees of physical activity of the individuals when the blood was drawn. On average, there were no significant differences in the serum level of MG53 protein in patients without diabetes and patients with diabetes ($P = 0.113$) (Fig. 2E). Moreover, a plot of serum MG53 levels as a function of fasting blood glucose did not reveal a correlation in pooled serum samples from patients without diabetes and patients with diabetes ($R^2 = 0.048$) (Fig. 2F). The demographic information for the patients for Fig. 2F is summarized in Table 1. Overall, this contrasts with the findings by Wu et al., who reported

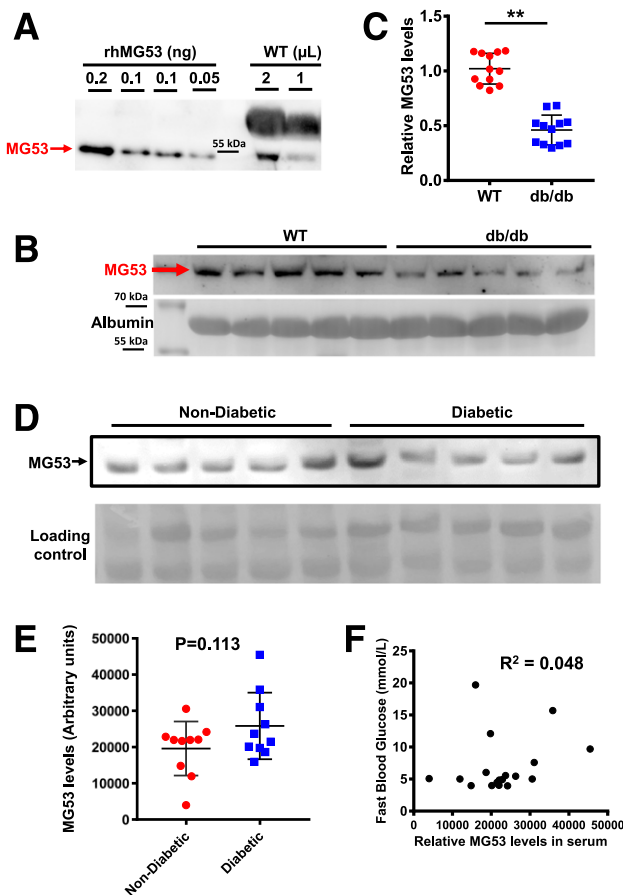


Figure 2—WBs detect lower or no change of serum MG53 levels in *db/db* mice or patients with diabetes compared with control subjects. **A**: 0.05–0.20 ng rhMG53 dissolved in *mg53*^{-/-} serum was used to establish the linear range for WB with the mAb-MG53, and 1 or 2 μL sera derived from the C57BL/6 mice was loaded onto the same gel. The WB was representative of 15 other samples. **B**: 1 μL sera derived from WT (lanes 1–5) and *db/db* littermates (lanes 6–10) (purchased from The Jackson Laboratory [age 14 weeks]) was probed with mAb-MG53. Loading control represents staining of albumin. **C**: Normalized WB intensities of MG53 in sera were plotted for individual animals. MG53 levels in *db/db* serum were significantly lower than those in WT serum (***P* < 0.001). **D**: 1 μL sera derived from human individuals without diabetes and with diabetes was probed with mAb-MG53. **E**: Scatter plot of MG53 levels in sera of humans without diabetes and with diabetes. No significant differences were observed between the two groups (*P* = 0.113). **F**: Plot of serum MG53 level vs. fasting blood glucose in both samples of humans without diabetes and samples of humans with diabetes revealed no correlation (*R*² = 0.048).

a positive correlation between MG53 and glucose levels in the human serum.

Muscle Atrophy in *db/db* Mice Contributes to Reduced Secretory Activity of MG53

Previously, Song et al. (14) published findings of higher MG53 protein content in muscle samples derived from mice with diabetes and human patients with diabetes, with a hypothetical role of MG53 serving as a causative factor for insulin resistance and diabetes. Their findings were not recapitulated by multiple independent investigators

(17–23). Indeed, many groups have shown that MG53 protein levels remain similar in muscle samples from healthy subjects and subjects with diabetes. We used the Abcam antibody and our mAb-MG53 antibody to quantify the protein level of MG53 in skeletal muscle derived from *db/db* and WT littermates. As shown in Fig. 3A, both Abcam and mAb-MG53 antibodies detected MG53 protein levels that are indistinguishable between *db/db* and WT muscle samples.

IHC staining was used to detect whether there were differences in subcellular distribution in *db/db* and WT mice. As shown in Fig. 3B, cross-sectional staining of gastrocnemius or soleus muscle showed similar patterns of MG53 distribution in WT and *db/db* mice. We found that *db/db* mice at the age of 4 months displayed remarkable muscle atrophy. The soleus muscle weight of the *db/db* mice was ~50% less than that of the WT littermates (Fig. 3C).

Following the protocol developed by Wu et al. (16), we used the soleus muscle bundle to determine the secretory activity of MG53 release in response to insulin stimulation. The amount of MG53 released into the bath media was quantified using our mAb-MG53 antibody. As shown in Fig. 3D (top panel), equal volume loading of the bathing solution from the individual soleus demonstrated significantly lower levels of MG53 from *db/db* soleus compared with the WT soleus. The reduced MG53 secretion was observed at all time points during the 2-h measurement (Fig. 3E). Interestingly, when sample loading was normalized to the soleus muscle mass, nearly identical time-dependent release of insulin-induced MG53 release was measured (Fig. 3D, bottom panel). Thus, insulin stimulation of MG53 muscle secretion was not different between WT and *db/db* muscle, whereas reduced muscle mass due to atrophy may be a contributing factor for the compromised level of MG53 in *db/db* serum.

MG53 Does Not Impact Glucose Hemostasis or Insulin Sensitivity in *db/db* Mice

The role of MG53 in the manifestation of insulin resistance and diabetes remains controversial. While Song et al. (14) and Wu et al. (16) hypothesize that MG53 can be a causative factor for the development of diabetes, presumably via downregulation of IRS-1, published studies by other investigators do not support their findings (17–23). Indeed, mice with ablation of IRS-1 lack a clear phenotype of type 2 diabetes.

If MG53 serves as causative factor for diabetes, whole-body ablation of MG53 in mice would be expected to delay the onset of the diabetic phenotype in the *db/db* background. For this purpose, we crossed the *db/db* mice with the *mg53*^{-/-} mice to evaluate growth pattern, glucose tolerance, and insulin sensitivity. As shown in Fig. 4A, we were surprised to find that the *db/db-mg53*^{-/-} mice behaved nearly identically to the *db/db* littermates during the 32-month observation period. We conducted GTT with the four mouse strains, WT, *mg53*^{-/-}, *db/db*, and

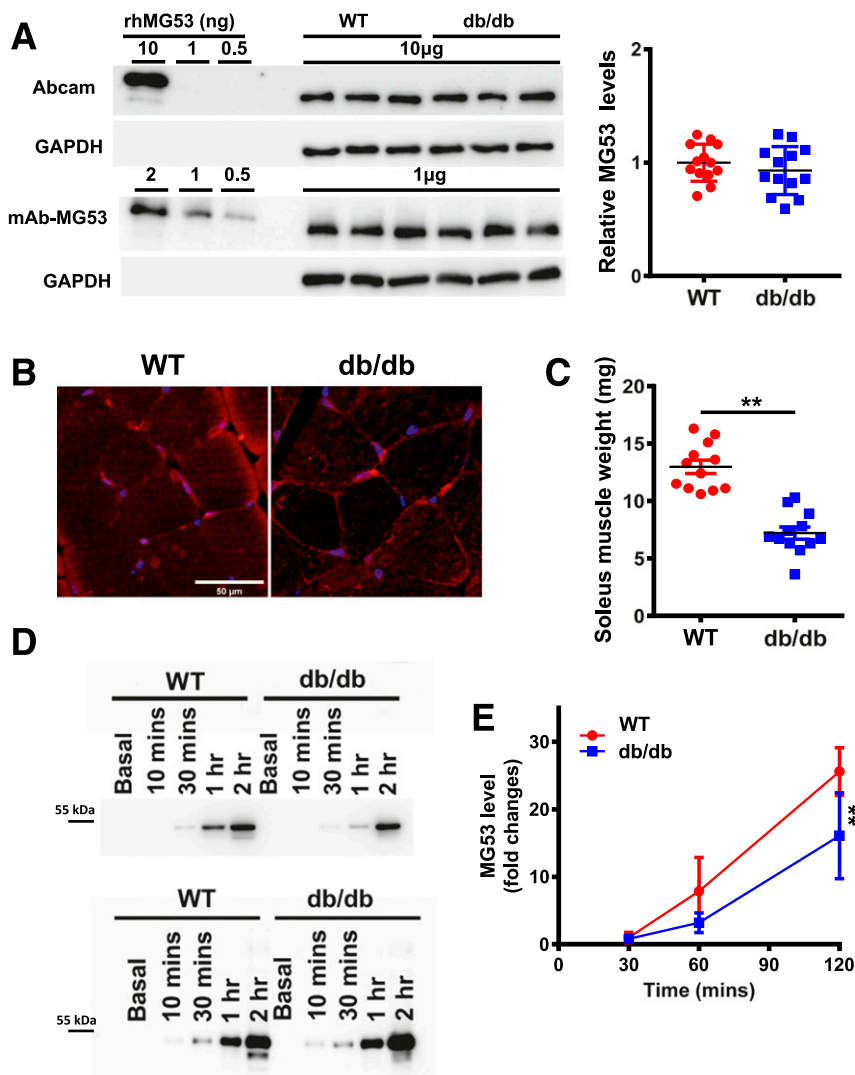


Figure 3—Muscle atrophy in *db/db* mice leads to reduced secretory activity of MG53. **A**: Skeletal muscles from WT and *db/db* littermate mice were probed with Abcam antibody (top) and mAb-MG53 (bottom). On average, there was no statistical difference in MG53 protein between WT and *db/db* muscle. **B**: Cross section of skeletal muscle derived from WT (left) and *db/db* (right) mice was stained with mAb-MG53. **C**: Comparison of soleus muscle mass derived from littermates of WT and *db/db* mice at 4 months of age (***P* < 0.01). **D**: 20 μL out of a total of 2 mL solution bathing the soleus was loaded onto the gel at different time points after insulin treatment (top). Smaller amounts of MG53 were detected from *db/db* soleus at all time points. The bottom panel shows loading of the bathing solution normalized to soleus muscle mass. **E**: Time-dependent secretion of MG53 from WT (red) or *db/db* (blue) soleus muscle following insulin treatment (***P* < 0.01).

db/db-mg53^{-/-}, at 18 weeks and 30 weeks of age (Fig. 4B). As expected, mice with the *db/db* background revealed glucose intolerance; interestingly, *db/db-mg53^{-/-}* and *db/db* showed indistinguishable time-dependent glucose clearance at 18 weeks of age. GTT of the *db/db-mg53^{-/-}* mice showed a trend of reduced glucose tolerance compared with *db/db* littermates, but the difference did not reach statistical significance. This finding suggests that ablation of MG53 did not have any benefits pertaining to, and in fact, may actually have worsened, the development of diabetes in mice.

We conducted ITT with the same mouse cohorts at 20 weeks and 32 weeks, respectively (Fig. 4C). Here again, we see that mice with ablation of MG53, either in the WT

or *db/db* background, do not show any improvement of insulin sensitivity; rather, a somewhat compromised insulin response was observed at both ages. Quantification of the AUC for the data shown in Fig. 4B supports the notion that ablation of MG53 in the *db/db* background had no impact on glucose handling at 18 weeks of age and trended toward worsened glucose handling at 30 weeks of age (Fig. 4D).

We next tested the hypothesis that elevation of MG53 in the serum may play a role in the development of insulin resistance and diabetes. Considering the proposal by Wu et al. (16) that anti-MG53 antibody used to sequester MG53 in the serum could have benefits to reduce blood glucose level in the *db/db* mice, we expect that sustained

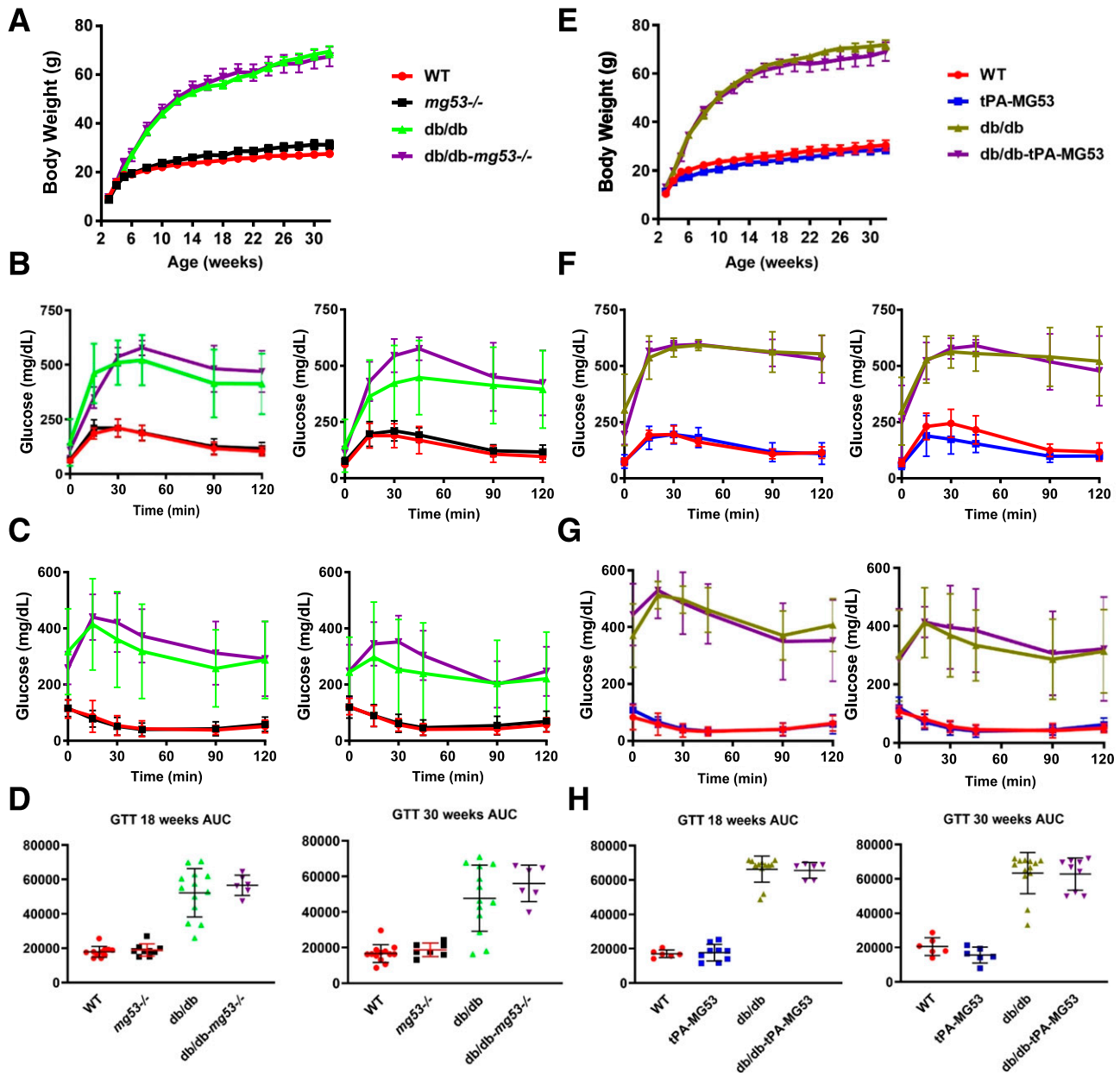


Figure 4—Neither ablation of MG53 nor elevation of MG53 impacts glucose hemostasis and insulin sensitivity in *db/db* mice. **A:** Body weight measurement of the four mice strains up to 32 weeks of age (WT, *n* = 13; *mg53*^{-/-}, *n* = 9; *db/db*, *n* = 12; and *db/db-mg53*^{-/-}, *n* = 6). These mice were littermates produced through crossbreeding of the *db*^{+/-} *mg53*^{+/-} pairs. **B:** GTT measurements at 18 weeks (left) and 30 weeks (right) (WT, *n* = 11; *mg53*^{-/-}, *n* = 9; *db/db*, *n* = 12; and *db/db-mg53*^{-/-}, *n* = 6). GTT of the *db/db-mg53*^{-/-} mice showed a trend of reduced glucose tolerance compared with *db/db* littermates, but the difference did not reach statistical significance. **C:** ITT measurements at 20 weeks (left) and 32 weeks (right) (WT, *n* = 11; *mg53*^{-/-}, *n* = 9; *db/db*, *n* = 12; and *db/db-mg53*^{-/-}, *n* = 6). **D:** Quantification of AUC for the data shown in **B**. **E:** Body weight of the WT, tPA-MG53, *db/db*, and *db/db-tPA-MG53* littermates was measured up to 32 weeks of age (WT, *n* = 7; tPA-MG53, *n* = 6; *db/db*, *n* = 7; and *db/db-tPA-MG53*, *n* = 5). **F:** GTT measurements at 18 weeks (left) and 30 weeks (right). **G:** ITT measurements at 20 weeks (left) and 32 weeks (right). Both sexes of mice were included in the experiments. **H:** Quantification of AUC for data shown in **F**.

elevation of MG53 in the serum would produce deleterious effects on the development of the *db/db* mice. We generated a transgenic mouse with muscle-derived secretion of MG53 into the bloodstream at a sustained level of ~100-fold higher than the basal level of MG53 detected in the WT mice (25). The tPA-MG53 mice lived a healthy life span, up to the age of 36 months. Therefore, we crossed

the tPA-MG53 mice with the *db/db* mice to evaluate whether sustained elevation of MG53 levels can alter GTT and ITT in the *db/db* mice. As shown in Fig. 4E, the growth pattern of tPA-MG53 is similar to that of the WT littermates; moreover, the *db/db* and *db/db-tPA-MG53* cohorts have similar growth patterns. This is surprising but not unexpected considering the following. In Fig. 4F,

we show data with GTT studies of the four mouse strains at 18 weeks and 30 weeks of age. There was no clear difference among the WT and tPA-MG53 littermates, or the *db/db* and the *db/db*-tPA-MG53 littermates, as illustrated in the quantification of AUC (Fig. 4G). When ITT was performed with the same mouse cohorts, there was again no significant difference between the WT and the tPA-MG53 pairs or the *db/db* and *db/db*-tPA-MG53 pairs (Fig. 4H).

Overall, we have tested both extremes of MG53 reduction and elevation in the *db/db* mice (e.g., with knock-out or overexpression) and have found no measurable impact on the handling of insulin signaling and glucose uptake in mice.

mg53^{-/-} Mice Show Compromised Glucose Handling After STZ Administration

Using an STZ-induced type 1 diabetes model (27), we compared the fasting blood glucose levels and GTT and ITT performance of the WT and *mg53*^{-/-} littermate mice. For this study, mice received five daily doses of STZ. At 1 week following the STZ treatment, the fasting blood glucose level remained in the normal range in both WT and *mg53*^{-/-} mice (Fig. 5A). Significant elevation of fasting blood glucose level was observed at 2 weeks post-STZ treatment, confirming the development of type 1 diabetes. GTT conducted at 2-weeks post-STZ treatment revealed a significant difference between the WT and *mg53*^{-/-} mice, indicating more severe dysfunction of glucose handling in the *mg53*^{-/-} mice (Fig. 5B). AUC measurement supports this notion (Fig. 5C). The ITT study was conducted at 3 weeks post-STZ treatment, which did not reveal any significant difference between the WT and *mg53*^{-/-} mice (Fig. 5D).

Compromised Corneal Wound Healing in *db/db* Mice Is Ameliorated With Systemic Administration of rhMG53 Protein

Chronic hyperglycemia in diabetes is associated with compromised tissue repair and regeneration in diabetes. Human patients with diabetes often develop oculopathy (29–34), and *db/db* mice have previously been used for oculopathy research. Following our published protocol of alkaline-induced ocular injury in mice (13), we found that *db/db* mice subjected to alkaline-induced ocular injury develop compromised reepithelialization, as measured by sustained fluorescein staining (Fig. 6A). With topical administration of rhMG53 protein (3 μ g/eye daily, topical volume of 30 μ L), reduced fluorescein staining was observed in the *db/db* cornea (Fig. 6A, bottom). The therapeutic effect of rhMG53 in facilitating reepithelialization of alkaline-induced injury to the cornea is summarized in Fig. 6B. Topical eye drop application of rhMG53 improved reepithelialization in the *db/db* cornea to a level that is better than that of the natural healing of the WT cornea.

We conducted IHC staining of flat mount cornea derived from the WT and *db/db* mice at 14 days post-alkaline-burn injury. While *db/db* cornea develop excessive

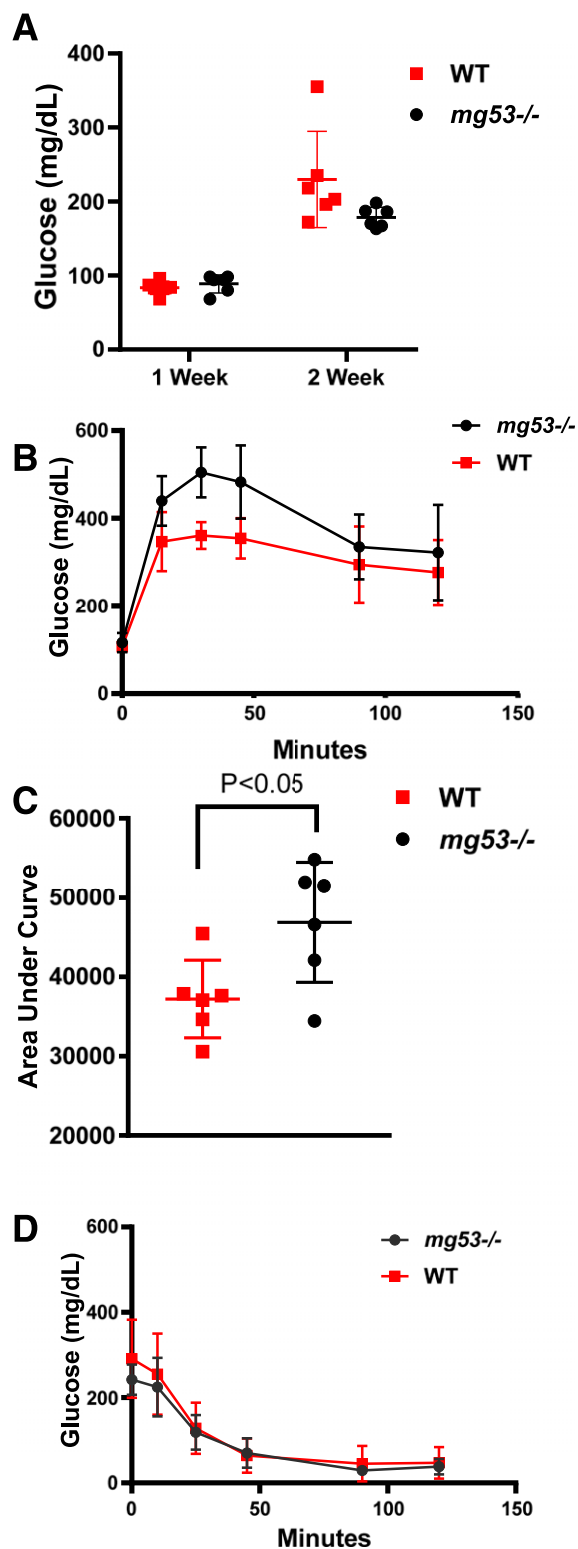


Figure 5—*mg53*^{-/-} mice show compromised glucose handling following STZ administration. **A:** Fasting blood glucose levels were measured at 1 and 2 weeks following the last dose of STZ injection. **B:** GTT was conducted at 2 weeks post-STZ. Significant differences were measured at 30 and 45 min ($P = 0.002$ and 0.008 , respectively). **C:** AUC measurement of **B** revealed significant differences between WT and *mg53*^{-/-} mice ($P = 0.025$). **D:** Three weeks post-STZ, ITT measurement revealed no significant difference between WT and *mg53*^{-/-} mice.

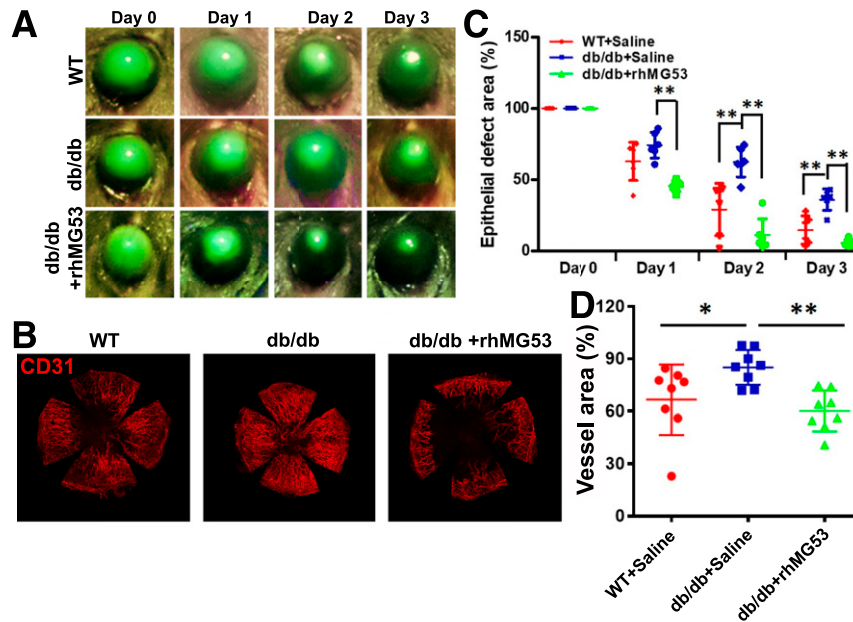


Figure 6—Compromised corneal wound healing in *db/db* mice is ameliorated with systemic administration of rhMG53 protein. *A*: Intensity of fluorescein staining at days 0–3 following alkaline injury to the cornea was presented for WT (top), *db/db* (middle), and *db/db* with rhMG53 treatment (bottom). *B*: Fluorescein intensity at different days after corneal alkaline injury was normalized to day 0. *db/db* cornea showed delayed healing of the cornea, which was improved with topical administration of rhMG53. *C*: Flat mounts of the cornea were stained with CD31 to reveal different degrees of vascularization at 14 days post-alkaline-induced injury to the cornea. *D*: Intensity of CD31 signal was used as index of vascularization of the cornea at 14 days post-alkaline injury (* $P < 0.05$; ** $P < 0.01$).

revascularization following alkaline injury compared with WT cornea, the addition of rhMG53 could ameliorate excess vascularization (Fig. 6C). The effects of MG53 on reduction of vascularization are statistically significant in the *db/db* cornea (Fig. 6D). These findings are consistent with our published observation that rhMG53 improves wound healing as well as suppresses fibrotic remodeling in the cornea (13). The data presented here further support the physiological role for MG53 in facilitating tissue repair and regeneration even in diabetic mice—rather than a role as a compromising factor for diabetes.

Repetitive Intravenous Administration of rhMG53 Did Not Alter Blood Metabolites in Rats

While our data shown in Fig. 6 support the therapeutic value of rhMG53 in treatment of ocular injury, the safety profile of rhMG53 must be assessed before we can proceed with further translational efforts. Our previous publications show that repetitive intravenous administration of rhMG53 in rodents and dogs did not produce adverse effects (6,8); however, we have not established the maximum tolerated dose for rhMG53 in animal models. Through collaboration with an independent contract research organization (SRI Biosciences), we conducted toxicology evaluation with rhMG53 in rats. Male and female rats at the age of 7–9 weeks were subjected to repetitive intravenous dosing on a daily basis. Clinical observations did not reveal any signs of abnormality with repetitive dosing up to 40 mg/kg. Thus, the maximum tolerated dose

is >40 mg/kg for MG53 in rats. Measurement of blood metabolites as shown in Table 2 did not reveal any signs of pathology in blood glucose, liver function (AST and alanine aminotransferase), or lipid metabolism (cholesterol and triglyceride). Only changes in glucose and triglycerides were observed with repetitive injection of the highest dose, 40 mg/kg rhMG53, in rats. This is not unexpected, as such dosing would be at least 40-fold higher than the therapeutic dose one would use in *in vivo* studies or human clinical trials.

DISCUSSION

We provide much evidence to show that MG53 does not participate in the manifestation of diabetes in mice. Specifically, neither whole-body ablation of MG53 nor sustained elevation of MG53 in the bloodstream impacted glucose handling in the *db/db* mice. Using a highly sensitive and specific mAb-MG53 antibody, we found that the MG53 level in serum derived from the *db/db* mice is significantly lower than that derived from the WT littermates as a result of a reduced capacity of skeletal muscle to secrete MG53 due to muscle atrophy. With a limited number of human serum samples, we found no evidence of correlation of glucose level and MG53 content in the serum. We further present data to show that rhMG53 has beneficial effects in treating alkaline-induced ocular injury in the *db/db* mice.

A series of studies published by Xiao and colleagues suggested MG53 might be a causative factor for diabetes

Table 2—Repetitive intravenous administration of rhMG53 did not alter blood metabolites in rats

	Male				Female			
	Control	1 mg/kg rhMG53	10 mg/kg rhMG53	40 mg/kg rhMG53	Control	1 mg/kg rhMG53	10 mg/kg rhMG53	40 mg/kg rhMG53
Blood urea nitrogen (mg/dL)	14.7 ± 1.5	14.7 ± 1.5	16.7 ± 1.5	16.0 ± 1.0	21.7 ± 4.0	22.7 ± 1.2	20.0 ± 3.6	18.7 ± 2.1
Creatinine (mg/dL)	0.190 ± 0.000	0.197 ± 0.021	0.220 ± 0.036	0.267 ± 0.015#	0.327 ± 0.049	0.333 ± 0.042	0.390 ± 0.082	0.407 ± 0.064
Glucose (mg/dL)	175 ± 4.4	173.3 ± 21.9	192.7 ± 16.3	258.3 ± 33.1*	176.7 ± 5.1	187.7 ± 8.6	184.0 ± 4.6	206.3 ± 6.8*
AST (units/L)	84.3 ± 12.9	81.3 ± 6.0	83.7 ± 10.0	74.7 ± 5.1	81.7 ± 20.2	74.7 ± 4.9	78.0 ± 5.6	77.7 ± 9.0
ALT (units/L)	58.3 ± 6.7	59.0 ± 6.2	62.0 ± 15.5	55.7 ± 0.6	52.7 ± 4.0	46.7 ± 3.8	47.3 ± 4.5	47.0 ± 6
Alkaline phosphatase (units/L)	368.3 ± 32.0	352.7 ± 63.3	394 ± 60.4	325.0 ± 47.6	199.0 ± 7.8	180.0 ± 20.2	171.3 ± 34.6	187.3 ± 11.9
Cholesterol (mg/dL)	89.3 ± 7.4	100 ± 16.5	80.3 ± 7.0	92.0 ± 5.2	81.3 ± 18.9	80.3 ± 16.3	89.3 ± 22.9	92.3 ± 3.8
Triglyceride (mg/dL)	149.0 ± 53.7	103.0 ± 38.4	75.7 ± 34.2	99.0 ± 51.7	126.7 ± 39.8	80.7 ± 16.0	40.3 ± 5.0*	48.3 ± 9.3*

Data are means ± SD. Male and female rats were dosed intravenously with rhMG53 (0, 1, 10, and 40 mg/kg daily). *n* = 3/group. Blood metabolites at the end of the 14 days' dosing were analyzed. ALT, alanine aminotransferase. **P* < 0.01. #*P* < 0.05.

(14–16). In the first article (14), Song et al. reported that the expression level of MG53 was significantly increased in animal models and human patients with diabetes. They proposed that upregulation of MG53 might cause insulin resistance via E3-ligase-mediated degradation of IRS-1. While two publications showed upregulation of MG53 in samples from diabetic rats (35,36), the larger majority of publications from multiple investigator groups failed to observe upregulation of MG53 in diabetic animals and humans (17–23). IRS-1 knockout mice do not develop diabetes (37,38) due to the compensatory function of other subtypes of IRS (39). A recently published proteomic study examined IRS-1 interaction proteins in skeletal muscle from normal individuals, obese insulin-resistant control subjects without diabetes, and patients with type 2 diabetes before and after insulin infusion (40). The work failed to identify any changes in MG53 protein interaction with IRS-1 across all groups. Thus, mounting evidence and the data presented here argue against the proposed role of MG53 in diabetes development.

In a follow-up study (15), a new role for MG53 modulation of PPAR α in cardiomyopathy was proposed. The authors generated transgenic mice using α MHC promoter to drive cardiac-specific overexpression of MG53 (α MHC-MG53). They found that cardiac overexpression of MG53 induced hypertrophy and cardiomyopathy, due to PPAR α -induced lipid toxicity. Interestingly, an independent study by Ham and Mahoney (41) using the same α -MHC promoter to drive cardiac overexpression of MG53 in mice reported a different cardiac phenotype. Ham and Mahoney showed that the α MHC-MG53 mice displayed cardiomyopathy at a young age when MG53 expression in the heart was already high. Only when the α MHC-MG53 mice grew older was a heart hypertrophic phenotype observed. However, even with sustained elevation of MG53 in the heart, the protein level of IRS-1 in the α MHC-MG53 mouse heart was rather high (above the level of the WT littermates) (41), which went against the notion that MG53 functions as an E3-ligase to degrade IRS-1, causing the development of diabetes (14). A more recent publication by Liu et al. (42) found that knockout of MG53 actually exacerbated pressure overload-induced heart hypertrophy, which would support an antihypertrophic function of MG53 instead.

Our group has generated an MG53 transgenic mouse line, which achieves sustained elevation of circulating MG53 by fusing of a tPA secretory peptide at the amino terminus of MG53 protein (tPA-MG53) (12,25). The tPA-MG53 mice maintained sustained elevation of MG53 in their bloodstream and lived a healthy life span with enhanced tissue repair and regeneration capacity (25). Here, we tested the hypothesis that sustained elevation of MG53 in circulation may impact the development of diabetes by crossing the *db/db* mice with the tPA-MG53 mice. We found that the *db/db*-tPA-MG53 mice did not develop exacerbated symptoms of diabetes, and their growth pattern, GTT, and ITT responses were similar to those of the *db/db* littermates. We also crossed the *db/db*

mice with the *mg53*^{-/-} mice and, again, did not observe any measurable changes in glucose handling or insulin signaling in the *db/db*-*mg53*^{-/-} mice. Together, our findings do not support a causative role for MG53 in promoting the development of type 2 diabetes.

A more recent publication by Wu et al. (16) proposed the use of anti-MG53 antibody to sequester circulating MG53 in the blood to treat diabetes in *db/db* mice (see also Zhu et al. [43]). The premise is that circulating level of MG53 is high in diabetic animals and human patients with type 2 diabetes, based on immunoblotting using both commercially available and their custom-made antibodies against MG53. In the current study, we demonstrate that the same commercial antibody (cat. no. 83302; Abcam) used by Wu et al. actually recognized nonspecific bands in serum derived from multiple strains of *mg53*^{-/-} mice. Thus, caution should be exercised when interpreting the identity and quantity of MG53 in the serum. Wu et al. reported that the basal level of MG53 in the blood was in the range of 200–300 pg/mL, which would be outside the range of detection with the use of available immunoblot methods. Our study demonstrates that the basal level of MG53 in the WT mice was in the range of 20–40 ng/mL, and the MG53 protein level was actually significantly lower in the *db/db* mice compared with the WT littermates (25). We conducted studies with a limited number of human patients with diabetes and found levels of MG53 protein in the serum similar to those from healthy volunteers. Admittedly, due to limited sample availability, the male-to-female ratio of the control group versus the group with diabetes is variable and we could not rule out sex variance. The large variations in the serum level of MG53 in healthy human patients and human patients with diabetes are due to the intrinsic nature of MG53—the circulating MG53 likely reflects the different exercise activity of the individual's skeletal muscle, which secretes MG53. Such larger variations of the serum MG53 are also reported by Wu et al. (16). The main point is that there is no correlation between MG53 content and glucose level in the human serum samples (not in healthy subjects or in subjects with diabetes). Taken together, our observations did not show a correlation of serum MG53 level and fast blood glucose levels. Furthermore, we found no correlation between the serum level of MG53 and fasting blood glucose in the human samples.

We followed the previously published protocol (16) to assess the capacity of insulin-induced secretion of MG53 from skeletal muscle derived from WT and *db/db* littermate mice. We were surprised to see that there was no sign of an exaggerated response of insulin-induced MG53 secretion from the diabetic mouse muscle. Rather, we found a reduced capacity of insulin-induced MG53 secretion in diabetic mouse muscle, which reflected the atrophic phenotype of skeletal muscle in the *db/db* mice. Thus, we conclude that muscle atrophy served as a contributing factor for the compromised level of MG53 in serum derived from the *db/db* mice.

Wu et al. tested the efficacy of their custom-made MG53 antibody to reduce blood glucose levels in the *db/db* mice. They found that intravenous injection of their anti-MG53 antibody (1.5 mg per mouse [or ~20–30 mg/kg]) led to a modest reduction of glucose level, from ~425 to 375 mg/dL (with an SE of <10 mg/dL) (Fig. 5C in the article by Wu et al.), marking this as a significant difference ($P < 0.01$). However, their supplementary data reported blood glucose level >600 mg/dL, which is ~175 mg/dL higher than data shown in the article under identical conditions (e.g., *db/db* mice receiving IgG as control) (16). One cannot conclude any beneficial effects of their anti-MG53 antibody in reducing glucose levels based on the available data. What is more, even if the 50 mg/dL reduction were realized, this reduction would not likely be clinically relevant, as that serum glucose level is still markedly high and likely to contribute to diabetic pathophysiology (43). The clinical impact of this finding from the murine model would need to be evaluated for safety and efficacy in humans.

Using STZ-induced acute diabetes in mice, we identified a potential role for MG53 in preservation of β -cell function under stress conditions. The *mg53*^{-/-} mice displayed a more severe dysfunction of glucose handling (GTT) compared with WT littermates at 2 weeks following STZ treatment, whereas ITT did not show significant difference between the WT and *mg53*^{-/-} littermates (Fig. 5). A trend for dysfunctional glucose handling was also observed with the *db/db* mice when crossed with the *mg53*^{-/-} mice (Fig. 4). Thus, it is possible that the absence of MG53 leads to increased susceptibility of β -cells to stress-induced injuries. Further experiments are required to elucidate the mechanistic base for MG53 in preservation of β -cell function as a potential means for using rhMG53 to treat type 1 diabetes.

Overall, data presented in the current study do not support any role of MG53 as a causative factor for the development of diabetes. We were not able to demonstrate evidence of MG53 elevation in serum derived from human patients with diabetes or in animal models of diabetes. We present data that show that repetitive systemic administration of rhMG53 did not alter glucose homeostasis or produce adverse effects in rodents (Table 2) or large animal models (6,8). The toxicology studies conducted in collaboration with an U.S. Food and Drug Administration–accredited contract research organization (CRO) provided strong evidence that repetitive intravenous administration of rhMG53 at levels >40-fold higher than the therapeutic dose did not cause a measurable impact on metabolic function or systemic vital organ toxicity. We did notice that the higher dose of 40 mg/kg rhMG53 (~570 μ g/mL) caused an increase in blood glucose in rats. However, this dose is >10,000-fold higher than the resting level of MG53 in the blood (~10–30 ng/mL). Such toxicity is expected for any therapeutic protein. Thus, we conclude that rhMG53 is potentially a safe and effective biologic to treat tissue injuries with no to limited impact on diabetogenesis. Regarding diabetic ophthalmopathy, we show that topical application of

rhMG53 produced beneficial effects in restoring ocular injuries in the *db/db* mice.

Our current study has several limitations. As diabetes is a complex metabolic disease, MG53 could also play a role in modulation of islet cell function, immune response, and multiple organ cross talk. While muscle atrophy may be a contributing factor for the reduction of circulating MG53 in diabetic animals, there are certainly other factors, such as reactive oxygen species, hyperglycemia, and chronic inflammation, which could compromise tissue repair and regeneration in diabetes. It is well-known that exercise has benefits to improve diabetes pathologies and promote MG53 secretion. Elucidating the molecular pathway(s) that facilitate exercise-mediated secretion of MG53 from skeletal muscle would be an important area of biomedical research in the future, which can provide alternative means for targeting muscle-tissue cross talk and cell-membrane repair to treat compromised organ function in metabolic diseases.

Funding. This work was supported by National Institutes of Health grants to B.A.W. (National Heart, Lung, and Blood Institute, R01HL143000), T.T. (National Institute of General Medical Sciences, R44GM123887), H.Z. (National Institute of Arthritis and Musculoskeletal and Skin Diseases, R01AR067766, and National Eye Institute, R01EY030621), and J.M. (National Institute on Aging, R01AG056919; National Institute of Diabetes and Digestive and Kidney Diseases, R01DK106394; and National Institute of Arthritis and Musculoskeletal and Skin Diseases, R01AR070752 and R01AR061385).

Duality of Interest. T.T. and J.M. have an equity interest in TRIM-edicine, Inc., which develops rhMG53 for treatment of human diseases. Patents on the use of MG53 are held by Rutgers University–Robert Wood Johnson Medical School. No other potential conflicts of interest relevant to this article were reported.

Author Contributions. Q.W., Z.B., Q.J., X.W., X.Z., K.H.P., and K.C. contributed to research data. W.H., B.A.W., H.L., C.C., T.T., and H.Z. contributed to discussion and reviewed and edited the manuscript. E.H. edited the manuscript. J.M. wrote the manuscript. J.M. is the guarantor of this work and, as such, had full access to all the data in the study and takes responsibility for the integrity of the data and the accuracy of the data analysis.

References

- Martinez RE, Quintana R, Go JJ, Villones MS, Marquez MA. Use of the WHO Package of Essential Noncommunicable Disease Interventions after Typhoon Haiyan. *Western Pac Surveill Response J* 2015;6(Suppl. 1):18–20
- Jeon CY, Murray MB. Diabetes mellitus increases the risk of active tuberculosis: a systematic review of 13 observational studies. *PLoS Med* 2008;5:e152
- Papaioannou D, Shen C, Nicolet D, et al. Prognostic and biological significance of the proangiogenic factor EGFL7 in acute myeloid leukemia. *Proc Natl Acad Sci U S A* 2017;114:E4641–E4647
- Schwarz PE, Gallein G, Ebermann D, et al. Global Diabetes Survey—an annual report on quality of diabetes care. *Diabetes Res Clin Pract* 2013;100:11–18
- Cai C, Masumiya H, Weisleder N, et al. MG53 nucleates assembly of cell membrane repair machinery. *Nat Cell Biol* 2009;11:56–64
- Weisleder N, Takizawa N, Lin P, et al. Recombinant MG53 protein modulates therapeutic cell membrane repair in treatment of muscular dystrophy. *Sci Transl Med* 2012;4:139ra85
- Jia Y, Chen K, Lin P, et al. Treatment of acute lung injury by targeting MG53-mediated cell membrane repair. *Nat Commun* 2014;5:4387
- Duann P, Li H, Lin P, et al. MG53-mediated cell membrane repair protects against acute kidney injury. *Sci Transl Med* 2015;7:279ra36

9. Li H, Duann P, Lin PH, et al. Modulation of wound healing and scar formation by MG53 protein-mediated cell membrane repair. *J Biol Chem* 2015;290:24592–24603
10. Liu J, Zhu H, Zheng Y, et al. Cardioprotection of recombinant human MG53 protein in a porcine model of ischemia and reperfusion injury. *J Mol Cell Cardiol* 2015;80:10–19
11. Zhu H, Hou J, Roe JL, et al. Amelioration of ischemia-reperfusion-induced muscle injury by the recombinant human MG53 protein. *Muscle Nerve* 2015;52:852–858
12. Yao Y, Zhang B, Zhu H, et al. MG53 permeates through blood-brain barrier to protect ischemic brain injury. *Oncotarget* 2016;7:22474–22485
13. Chandler HL, Tan T, Yang C, et al. MG53 promotes corneal wound healing and mitigates fibrotic remodeling in rodents. *Commun Biol* 2019;2:71
14. Song R, Peng W, Zhang Y, et al. Central role of E3 ubiquitin ligase MG53 in insulin resistance and metabolic disorders. *Nature* 2013;494:375–379
15. Liu F, Song R, Feng Y, et al. Upregulation of MG53 induces diabetic cardiomyopathy through transcriptional activation of peroxisome proliferation-activated receptor α . *Circulation* 2015;131:795–804
16. Wu HK, Zhang Y, Cao CM, et al. Glucose-sensitive myokine/cardiokine MG53 regulates systemic insulin response and metabolic homeostasis. *Circulation* 2019;139:901–914
17. Ma H, Liu J, Bian Z, et al. Effect of metabolic syndrome on mitsugumin 53 expression and function. *PLoS One* 2015;10:e0124128
18. Ma LL, Kong FJ, Guo JJ, et al. Hypercholesterolemia abrogates remote ischemic preconditioning-induced cardioprotection: role of reperfusion injury salvage kinase signals. *Shock* 2017;47:363–369
19. Ma LL, Zhang FJ, Qian LB, et al. Hypercholesterolemia blocked sevoflurane-induced cardioprotection against ischemia-reperfusion injury by alteration of the MG53/RISK/GSK3 β signaling. *Int J Cardiol* 2013;168:3671–3678
20. Xu Y, Ma LL, Zhou C, et al. Hypercholesterolemic myocardium is vulnerable to ischemia-reperfusion injury and refractory to sevoflurane-induced protection. *PLoS One* 2013;8:e76652
21. Yi JS, Park JS, Ham YM, et al. MG53-induced IRS-1 ubiquitination negatively regulates skeletal myogenesis and insulin signalling. *Nat Commun* 2013;4:2354
22. Yuan H, Niu Y, Liu X, Yang F, Niu W, Fu L. Proteomic analysis of skeletal muscle in insulin-resistant mice: response to 6-week aerobic exercise. *PLoS One* 2013;8:e53887
23. Zabielski P, Lanza IR, Gopala S, et al. Altered skeletal muscle mitochondrial proteome as the basis of disruption of mitochondrial function in diabetic mice. *Diabetes* 2016;65:561–573
24. Peng BY, Wang Q, Luo YH, He JF, Tan T, Zhu H. A novel and quick PCR-based method to genotype mice with a leptin receptor mutation (*db/db* mice). *Acta Pharmacol Sin* 2018;39:117–123
25. Bian Z, Wang Q, Zhou X, et al. Sustained elevation of MG53 in the bloodstream increases tissue regenerative capacity without compromising metabolic function. *Nat Commun* 2019;10:4659
26. Anderson C, Zhou Q, Wang S. An alkali-burn injury model of corneal neovascularization in the mouse. *J Vis Exp* 2014;86:e51159
27. Nicholas SB, Aguiniga E, Ren Y, et al. Plasminogen activator inhibitor-1 deficiency retards diabetic nephropathy. *Kidney Int* 2005;67:1297–1307
28. Adesanya TMA, Russell M, Park KH, et al. MG 53 protein protects aortic valve interstitial cells from membrane injury and fibrocalcific remodeling. *J Am Heart Assoc* 2019;8:e009960
29. Jiang QW, Kaili D, Freeman J, et al. Diabetes inhibits corneal epithelial cell migration and tight junction formation in mice and human via increasing ROS and impairing Akt signaling. *Acta Pharmacol Sin* 2019;40:1205–1211
30. Ljubimov AV, Saghizadeh M. Progress in corneal wound healing. *Prog Retin Eye Res* 2015;49:17–45
31. Markoulli M, Flanagan J, Tummanapalli SS, Wu J, Willcox M. The impact of diabetes on corneal nerve morphology and ocular surface integrity. *Ocul Surf* 2018;16:45–57
32. Misra SL, Braatvedt GD, Patel DV. Impact of diabetes mellitus on the ocular surface: a review. *Clin Exp Ophthalmol* 2016;44:278–288
33. Shih KC, Lam KS, Tong L. A systematic review on the impact of diabetes mellitus on the ocular surface. *Nutr Diabetes* 2017;7:e251
34. Xu KP, Li Y, Ljubimov AV, Yu FS. High glucose suppresses epidermal growth factor receptor/phosphatidylinositol 3-kinase/Akt signaling pathway and attenuates corneal epithelial wound healing. *Diabetes* 2009;58:1077–1085
35. Qi J, Yang B, Ren C, Fu J, Zhang J. Swimming exercise alleviated insulin resistance by regulating tripartite motif family protein 72 expression and AKT signal pathway in Sprague-Dawley rats fed with high-fat diet. *J Diabetes Res* 2016;2016:1564386
36. Reddy SS, Shruthi K, Prabhakar YK, Sailaja G, Reddy GB. Implication of altered ubiquitin-proteasome system and ER stress in the muscle atrophy of diabetic rats. *Arch Biochem Biophys* 2018;639:16–25
37. Tamemoto H, Kadowaki T, Tobe K, et al. Insulin resistance and growth retardation in mice lacking insulin receptor substrate-1. *Nature* 1994;372:182–186
38. Terauchi Y, Iwamoto K, Tamemoto H, et al. Development of non-insulin-dependent diabetes mellitus in the double knockout mice with disruption of insulin receptor substrate-1 and beta cell glucokinase genes. Genetic reconstitution of diabetes as a polygenic disease. *J Clin Invest* 1997;99:861–866
39. Laustsen PG, Michael MD, Crute BE, et al. Lipoatrophic diabetes in *Irs1(-)/Irs3(-)* double knockout mice. *Genes Dev* 2002;16:3213–3222
40. Caruso M, Ma D, Msallaty Z, et al. Increased interaction with insulin receptor substrate 1, a novel abnormality in insulin resistance and type 2 diabetes. *Diabetes* 2014;63:1933–1947
41. Ham YM, Mahoney SJ. Compensation of the AKT signaling by ERK signaling in transgenic mice hearts overexpressing TRIM72. *Exp Cell Res* 2013;319:1451–1462
42. Liu W, Wang G, Zhang C, et al. MG53, a novel regulator of KCHIP2 and $I_{to,f}$, plays a critical role in electrophysiological remodeling in cardiac hypertrophy. *Circulation* 2019;139:2142–2156
43. Zhu H, Hsueh W, Whitson BA. Letter by Zhu et al regarding article, “Glucose-sensitive myokine/cardiokine MG53 regulates systemic insulin response and metabolic homeostasis”. *Circulation* 2019;140:e186–e187